



# DPP based dual-sensing probe for the multi-color detection of toxic $\text{Co}^{2+}$ / $\text{Sn}^{2+}$ and $\text{CN}^-$ ions in water: An electronic eye development

Ramalingam Manivannan<sup>1</sup>, Jiwon Ryu<sup>1</sup>, Young-A Son<sup>\*</sup>

Department of Advanced Organic Materials Engineering, Chungnam National University, 220 Gung-dong, Yuseong-gu, Daejeon, 305-764, South Korea

## ARTICLE INFO

### Keywords:

Electronic eye  
DPP  
Dual mechanism  
Multi-color  
Toxic ions

## ABSTRACT

A dual-sensing mechanism probe for the multi-color detection of toxic  $\text{Co}^{2+}/\text{Sn}^{2+}$  and  $\text{CN}^-$  ions in water based on a diketopyrrolopyrrole (DPP) moiety was designed and successfully synthesized. Colorimetric and fluorimetric methods were used to confirm the sensing performance of the probe. Different colors were achieved for the detecting ions  $\text{Co}^{2+}$ ,  $\text{Sn}^{2+}$ , and  $\text{CN}^-$ . pink for  $\text{Co}^{2+}$ , red for  $\text{Sn}^{2+}$ , and colorless for  $\text{CN}^-$ , denoting high selectivity in the developed probe. A dual-sensing mechanism confirmed for the metal ion the sensing is via complexation resulting in color (different) change through metal to ligand charge-transfer transition (MLCT), and for anion (cyanide), it is through addition reaction with a disconnection in intramolecular charge-transfer transition (ICT). Pre-added selected ions to the different water samples effectively detect different colors. We developed an electronic eye (RGB - Arduino device) for the detection of toxic ions effectively.

## 1. Introduction

Toxic ions, either anion or cations, have enormous effects in the biotic environment. The presence of ions and their detection in water is of primary importance from an industrial point of view and the environmental and biological system and the detection to be fast, reliable, and cost less [1–10]. The presence of metal ions ( $\text{Al}^{3+}$ ,  $\text{Co}^{2+}$ ,  $\text{Cr}^{2+}$ ,  $\text{Cu}^{2+}$ ,  $\text{Sn}^{2+}$ ,  $\text{Hg}^{2+}$ ,  $\text{Fe}^{2+}$ ,  $\text{Fe}^{3+}$ ,  $\text{Mg}^{2+}$ ,  $\text{K}^+$ ,  $\text{Na}^+$ ,  $\text{Ni}^{2+}$ , etc.) in excess or deficiency can lead to numerous physical complaints to the individual upon exposure. Simple anions like acetate, bromide, chloride, cyanide, fluoride, iodide, nitrate, and phosphate were well thought out as acute anions due to their significance in drinking water and resulting in disease onset when present in grater concentrations [11–13].  $\text{Co}^{2+}$  is a necessary element for life in trace amount and present in vitamin B<sub>12</sub> [14,15]. However, cobalt ingestion causes severe health issues like skin, respiratory problems, and even cancer, as per reports by the international agency for research on cancer, cobalt poisoning [16]. Thus the detection of even trace amounts of cobalt ion in water also significant. The insufficiency of  $\text{Co}^{2+}$  ions in human beings leads to hypothyroidism, anemia, and the chance to develop abnormalities in infants [17,18]. Amongst several cations, the detection of the  $\text{Sn}^{2+}$  ions is also equally crucial as certain organotin compounds are toxic like cyanide, when excess tin ion handled for a longer duration, which can quickly,

accumulates in kidney and liver and can cause serious problem to human health. The World Health Organization's tolerable bounds for the presence of tin ion in tinned food is 0.25 g/kg [19].

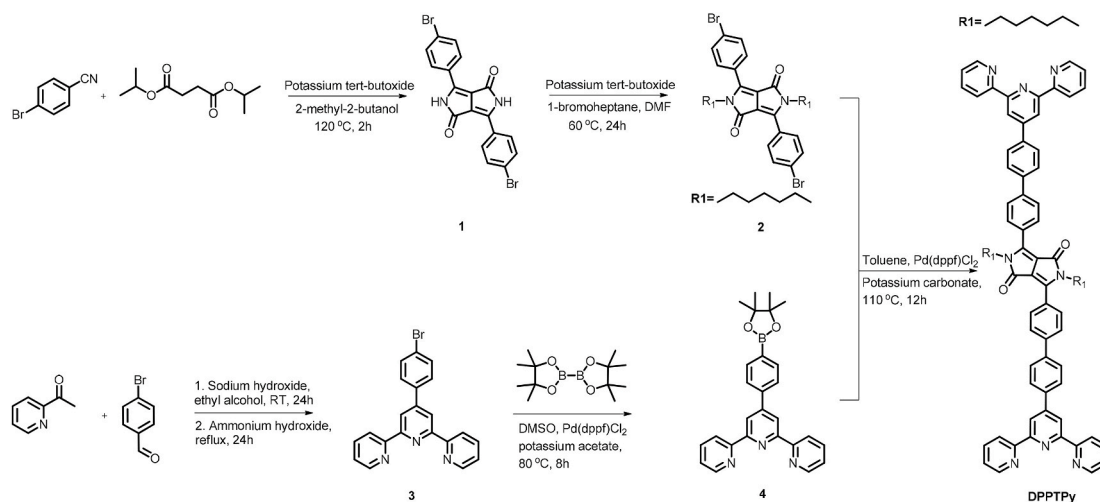
Of the many anions, cyanide is the most toxic and is of specific concern due to the daring poisonousness for the public and environment [20,21]. The preoccupation of cyanide ions through the skin, gastrointestinal tract, and lungs injures human health by vomiting, loss of consciousness, convulsion, and finally, death [22–24]. Nevertheless, the mandatory usage of cyanide in various fields like electroplating, gold mining, tanning, metallurgy, plastics manufacturing, and synthetic fibers makes the essential for the quantification and recognition of cyanide [25–30]. The WHO permits an extreme allowable limit of cyanide in drinking water is of 1.9  $\mu\text{M}$  [31]. Therefore, metal ions toxic to biological system detection using a chemical probe is of great importance.

In past years, various approaches available in the literature for ion detection like electrochemical detection methods, nanomaterials to detect via fluorescence changes, high-performance liquid chromatography, atomic absorption spectral technique, etc. Even though the result obtained are reliable and reproducible the techniques have some disadvantages as if detection procedure is time-consuming and expensive [32–37]. As a result, there exists a demand for the chemical sensor, which can have the ability to sense the ions with high selectivity. The colorimetric probe solves problems like expensive and time-consuming

<sup>\*</sup> Corresponding author.

E-mail address: [yason@cnu.ac.kr](mailto:yason@cnu.ac.kr) (Y.-A. Son).

<sup>1</sup> These authors contributed equally to this work.



Scheme 1. Synthesis of the probe, DPPTPy.

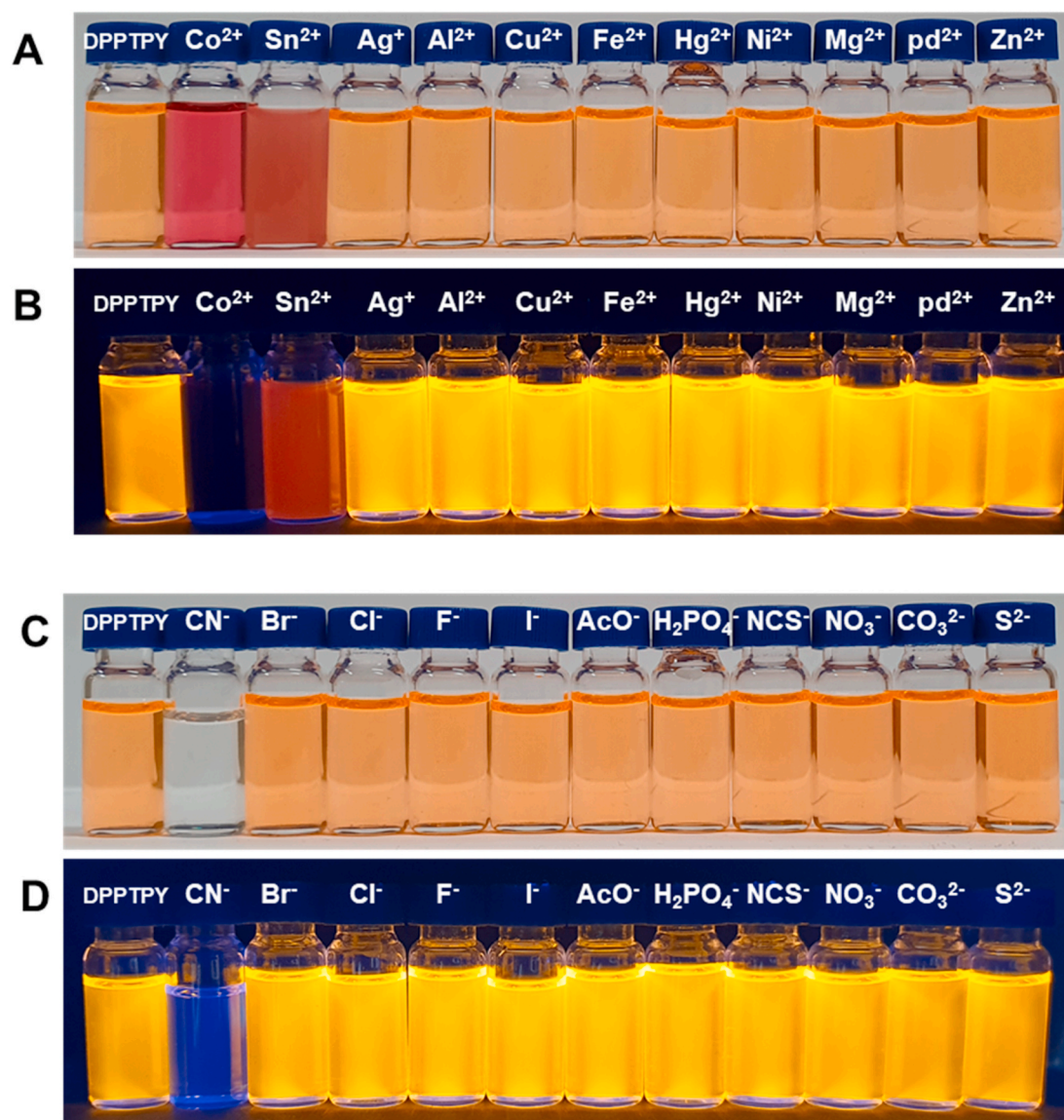


Fig. 1. Visual response of DPPTPY ( $2 \times 10^{-5}$  M) in day and fluorescent lamp in the presence of various cations (A, B) ( $2 \times 10^{-5}$  M) and anions (C, D) ( $2 \times 10^{-5}$  M) in 1:1 v/v DMF/H<sub>2</sub>O.

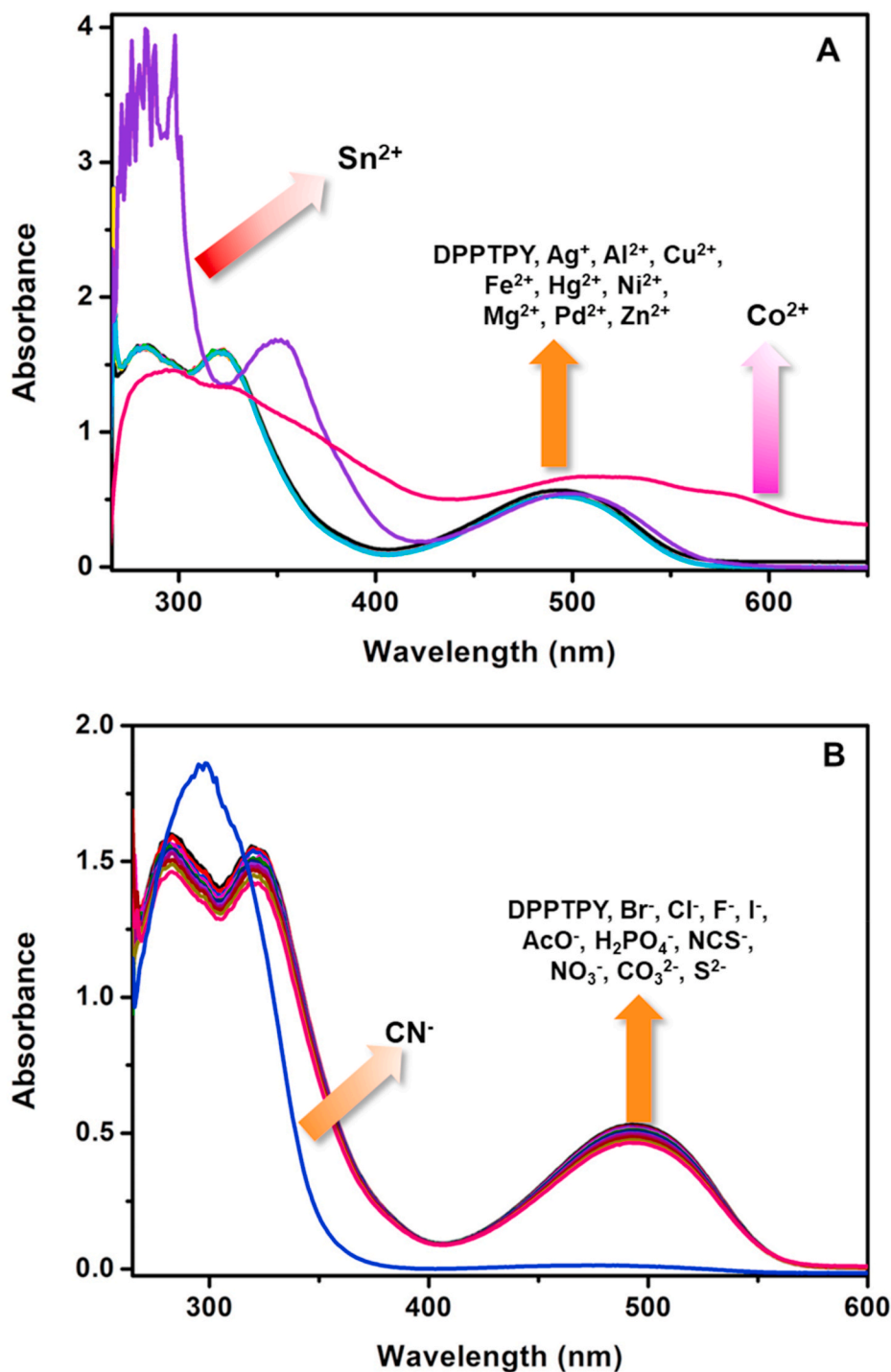


Fig. 2. UV-Visible response of DPPTPY [ $2 \times 10^{-5}$  M] in the existence of different cations [ $2 \times 10^{-5}$  M] (A) and anions [ $2 \times 10^{-5}$  M] (B) in 1:1 v/v DMF/ $\text{H}_2\text{O}$ .

and is used effectively for naked-eye detection of various ions present in the water medium [38–41].

Using these thoughts, herein we develop a diketopyrrolopyrrole (DPP) and terpyridine (TPy) based probe DPPTPy for the recognition of  $\text{CN}^-$  ions and metal cations ( $\text{Co}^{2+}$ ,  $\text{Sn}^{2+}$ ). The foremost objective was to synthesize a probe with intramolecular charge transfer (ICT) for  $\text{CN}^-$  ions in an aqueous media. The probe displays both fluorescent and absorption change with  $\text{CN}^-$  ion. As predicted, the probe, once treated by  $\text{CN}^-$  ion, would be exploited as a discerning fluorimetric and colorimetric probe for  $\text{CN}^-$  ions in aqueous media, diketopyrrolopyrrole (DPP) core in moiety acts to serve the need of sensing cyanide ion. For

metal ion ( $\text{Co}^{2+}$ ,  $\text{Sn}^{2+}$ ) detection in water terpyridine (TPy) core attached in the moiety, the two metal ions were detected with different color changes.

## 2. Experimental division

### 2.1. Materials and instruments

Compounds aimed at preparing DPPTPy: intermediate chemical, solvents, and cations (chloride salts), anion (tetra butyl ammonium salts) used for complete study acquired in sigma aldrich, tokyo chemical

industries, used without any further refinement. Distilled water is used for complete experiments. Proton and carbon-NMR of DPPTPy and its intermediates measured and confirmed on a Bruker 600 instrument. Mass analysis is done in JMS 700 JEOL spectrometer. Fluorescence and UV-Visible data were obtained in a Varian Cary Eclipse spectrophotometer and Agilent 8453 device, respectively. Slit widths for excitation/emission kept a constant of 3 nm throughout the experiment. The complete study for detecting anions and cations in this work is done in neutral pH conditions.

## 2.2. Synthesis and characterization of 3,6-Bis(4-bromophenyl)pyrrolo[3,4-c]pyrrole-1,4(2H,5H)-dione (1)

4-bromobenzonitrile (5 g, 27.5 mmol) in 2-methyl-2-butanol (20 mL) was added potassium t-butoxide (3.54 g, 31.5 mmol), the reaction mixture stirred for 30 min at 120 °C. To the reaction mixture, added in drops for 1 h a solution of diisopropyl succinate (2.22 g, 11 mmol) in 2-methyl-2-butanol (10 mL) and stirred for another 2 h at 120 °C. Then the reaction mixture cooled and added methanol (200 mL) and HCl (10 mL) solution mixture to the reaction, and the precipitate was filtered and washed with cold methanol (2 × 100 mL) and water (2 × 100 mL) to obtain pure compound as red solid (Yield 4.0 g, 81.7%). The obtained solid is insoluble; therefore, next step proceeded without characterization.

## 2.3. Synthesis and characterization of 3,6-Bis(4-bromophenyl)-2,5-diheptylpyrrolo[3,4-c]pyrrole-1,4(2H,5H)-dione (2)

3,6-bis(4-bromophenyl)pyrrolo[3,4-c]pyrrole-1,4(2H,5H)-dione (1 g, 2.25 mmol), potassium t-butoxide (0.5 g, 4.5 mmol) in DMF (25 mL) were mixed. Maintained 1 h room temperature stirring under a nitrogen atmosphere and then heated to 60 °C. 1-bromoheptane (excess about 10 equivalent) in DMF (10 mL) added in drops to the reaction mixture. Stirring continued for another 24 h, and then the reaction mixture cooled and added ethyl acetate to it and washed with water thrice (100 mL). The crude material was column purified using ethyl acetate and hexane as eluent to obtain a bright orange solid powder (yield 0.38 g, 26.4%). Melting point: 134–136 °C; FT-IR (KBr) ( $\nu_{\max}/\text{cm}^{-1}$ ): 2922, 2849, 1661, 1609, 1483, 1355, 1089, 1003, 843, 735, 672 (Fig. S1).  $^1\text{H}$  NMR (600 MHz  $\text{CDCl}_3$ ): 0.75 (t, 3H,  $J = 6.6$  Hz), 1.13 (m, 16H), 1.47 (s, 4H), 3.63 (t, 4H, 7.2 Hz), 7.57 (d, 8H, 7.2 Hz) (Fig. S2).  $^{13}\text{C}$  NMR (150 MHz  $\text{CDCl}_3$ ):  $\delta$  12.9, 21.4, 25.6, 27.6, 28.3, 30.5, 40.8, 108.9, 124.7, 125.9, 129.0, 131.2, 146.4, 161.3 (Fig. S3). HRMS ( $m/z$ ) calcd. for (Bromine isotope  $^{81}\text{Br}$ )  $\text{C}_{32}\text{H}_{39}\text{BrN}_2\text{O}_2$   $[\text{M}+\text{H}]^+$ : 643.1358, found 643.1361 (Fig. S4).

## 2.4. Synthesis and characterization of 4'-(4-Bromophenyl)-2,2':6',2''-terpyridine (3)

4-bromobenzaldehyde (3 g, 16.2 mmol) in ethyl alcohol (60 mL) solution was added 2-acetylpyridine (3.9 g, 32.4 mmol). To the stirred reaction mixture, sodium hydroxide (1.3 g, 32.4 mmol) was added, and the reaction mixture stirred at room temperature under a nitrogen atmosphere for 24 h and then added aqueous ammonia solution (28%, 60 mL) and refluxed for 24 h. After completing the reaction, cooled the reaction mixture and washed with cold ethanol (3 × 50 mL) to obtain pure product as a white solid (Yield 4.25 g, 67.5%). Melting point: 132–134 °C; FT-IR (KBr) ( $\nu_{\max}/\text{cm}^{-1}$ ): 3249, 1581, 1471, 1377, 1073, 823, 785, 734 (Fig. S5).  $^1\text{H}$  NMR (600 MHz  $\text{DMSO}-d_6$ ): 7.52 (m, 2H), 7.77 (d, 2H,  $J = 8.4$  Hz), 7.89 (d, 2H,  $J = 8.4$  Hz), 8.02 (m, 2H), 8.66 (d, 2H,  $J = 7.8$  Hz), 8.69 (s, 2H), 8.76 (d, 2H,  $J = 4.2$  Hz) (Fig. S6).  $^{13}\text{C}$  NMR (150 MHz  $\text{DMSO}-d_6$ ):  $\delta$  118.2, 121.4, 123.5, 125.0, 129.5, 132.7, 137.1, 137.9, 148.7, 149.8, 155.2, 156.2 (Fig. S7). HRMS ( $m/z$ ) calcd. for (Bromine isotope  $^{79}\text{Br}$ )  $\text{C}_{21}\text{H}_{15}\text{BrN}_3$   $[\text{M}+\text{H}]^+$ : 388.0449, found 388.0451 (Fig. S8).

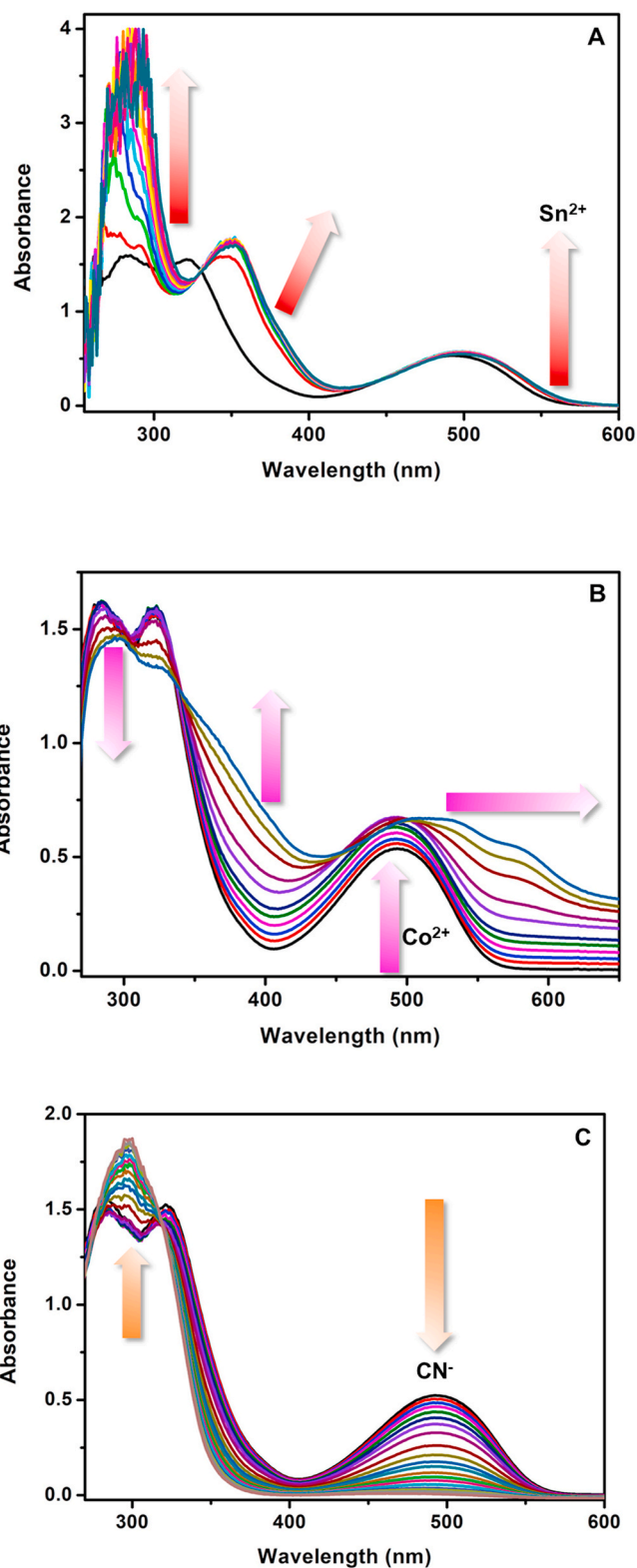


Fig. 3. UV-Visible spectra of DPPTPY [ $2 \times 10^{-5}$  M] in the presence of (A)  $\text{Sn}^{2+}$  [ $0-2 \times 10^{-5}$  M], (B)  $\text{Co}^{2+}$ , and (C)  $\text{CN}^-$  [ $0-2 \times 10^{-5}$  M] in 1:1 v/v DMF/ $\text{H}_2\text{O}$ .

## 2.5. Synthesis and characterization of 4'-(4-(4,4,5,5-tetramethyl-1,3,2-dioxaborolan-2-yl)phenyl)-2,2':6',2''-terpyridine (4)

4'-(4-bromophenyl)-2,2':6',2''-terpyridine (2.0 g, 5.15 mmol), bis (pinacolato)diboron (1.376 g, 5.419 mmol) in DMSO (20 mL) was added

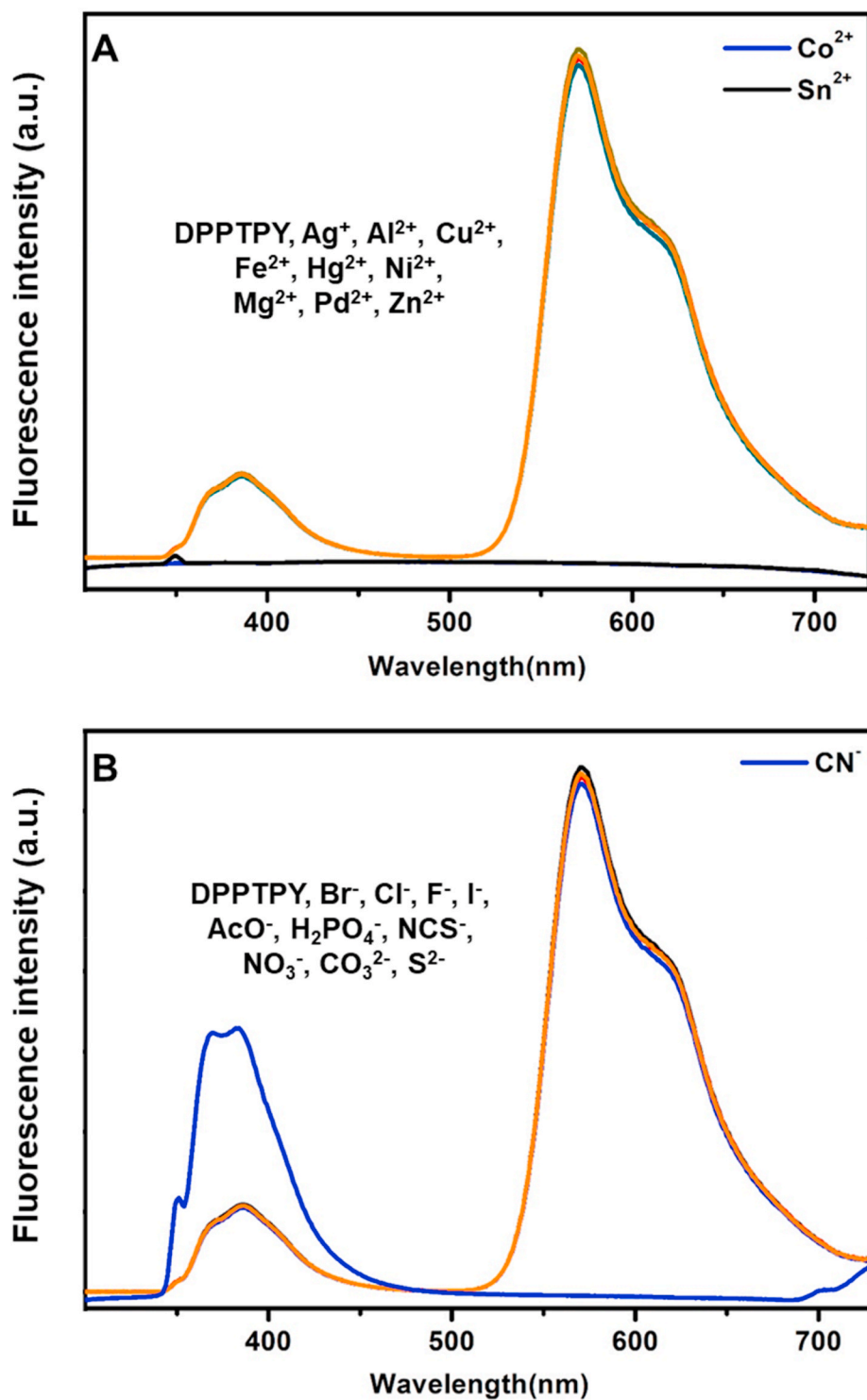


Fig. 4. Fluorescence spectra of DPPTPY [ $2 \times 10^{-5}$  M] in the existence of different cations [ $2 \times 10^{-5}$  M] (A) and anions [ $2 \times 10^{-5}$  M] (B) in 1:1 v/v DMF/H<sub>2</sub>O.

potassium acetate (1.516 g, 15.44 mmol). Then the reaction mixture degassed for 10 min under a nitrogen atmosphere and added Pd(dppf) Cl<sub>2</sub> (0.128 g, 0.18 mmol), then stirring continued at 80 °C for 8 h, toluene added to the reaction mixture and extracted with water. The process repeated twice, separated the organic layer, dried in sodium sulfate, and evaporated to obtain pure compound as white solid (yield 0.94 g, 42%). Melting point: 198–200 °C; FT-IR (KBr) ( $\nu_{\max}/\text{cm}^{-1}$ ):

3379, 1566, 1462, 1385, 1069, 790, 737 (Fig. S9). <sup>1</sup>H NMR (600 MHz CDCl<sub>3</sub>): 1.31 (s, 12H), 7.27 (m, 2H), 7.79 (m, 2H), 7.84 (m, 4H), 8.59 (d, 2H,  $J = 7.8$  Hz), 8.66 (m, 4H) (Fig. S10). <sup>13</sup>C NMR (150 MHz CDCl<sub>3</sub>):  $\delta$  23.8, 82.9, 117.9, 120.3, 122.8, 125.5, 134.3, 135.8, 139.9, 148.1, 149.1, 154.9, 155.2 (Fig. S11). HRMS ( $m/z$ ) calcd. for C<sub>27</sub>H<sub>27</sub>BN<sub>3</sub>O<sub>2</sub> [M+H]<sup>+</sup>: 436.2196, found 436.2160 (Fig. S12).

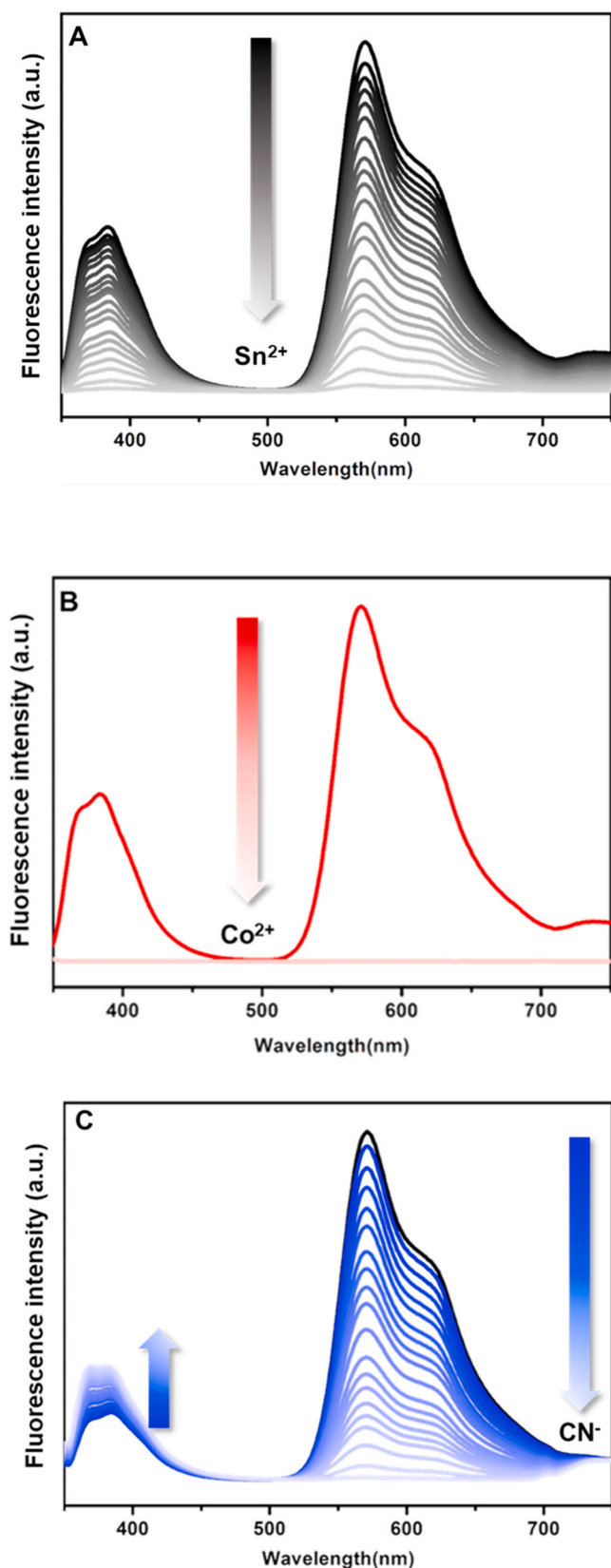


Fig. 5. Fluorescence spectra of DPPTPy [ $2 \times 10^{-5}$  M] in the presence of (A)  $\text{Sn}^{2+}$  [ $0.2 \times 10^{-5}$  M], (B)  $\text{Co}^{2+}$ , and (C)  $\text{CN}^-$  [ $0.2 \times 10^{-5}$  M] in 1:1 v/v DMF/ $\text{H}_2\text{O}$ .

## 2.6. Synthesis and characterization of 3,6-Bis(4'-([2,2':6',2''-terpyridin]-4'-yl)-[1,1'-biphenyl]-4-yl)-2,5-diheptylpyrrolo[3,4-c]pyrrole-1,4(2H,5H)-dione (DPPTPy)

4'-(4-(4,4,5,5-tetramethyl-1,3,2-dioxaborolan-2-yl)phenyl)-2,2':6',2''-terpyridine (0.4 g, 0.92 mmol), 3,6-bis(4-bromophenyl)-2,5-diheptylpyrrolo[3,4-c]pyrrole-1,4(2H,5H)-dione (0.16 g, 0.25 mmol), in toluene (20 mL) was added potassium carbonate (0.28 g, 2.68 mmol). Then the reaction mixture degassed for 10 min under nitrogen atmosphere. Added  $\text{Pd}(\text{dppf})\text{Cl}_2$  (0.037 g, 0.05 mmol), then stirring continued at  $110^\circ\text{C}$  for 12 h. Then the reaction mixture cooled to room temperature, added water (50 mL) to the reaction mixture extracted with dichloromethane ( $3 \times 100$  mL) and dried over sodium sulfate and recrystallized the crude material with methanol to obtain pure compound as brown solid (yield 0.23 g, 81%) and the overall yield obtained is 4.95%. Melting point:  $296\text{--}298^\circ\text{C}$ ; FT-IR (KBr) ( $\nu_{\text{max}}/\text{cm}^{-1}$ ): 2920, 1661, 1575, 1381, 1084, 791, 739, 624 (Fig. S13).  $^1\text{H}$  NMR (600 MHz  $\text{CDCl}_3$ ) 0.76 (t, 6H,  $J = 7.2$  Hz), 1.18 (m, 16H), 1.55 (m, 4H), 3.77 (bs, 4H), 7.27 (d, 4H,  $J = 5.4$  Hz), 7.71 (m, 8H), 7.78 (m, 4H), 7.88 (d, 4H,  $J = 7.2$  Hz), 7.94 (d, 4H, 7.8 Hz), 8.58 (d, 4H,  $J = 7.2$  Hz), 8.65 (s, 4H), 8.70 (s, 4H) (Fig. S14).  $^{13}\text{C}$  NMR (150 MHz  $\text{CDCl}_3$ ):  $\delta$  13.0, 21.5, 25.7, 27.7, 28.4, 28.6, 30.6, 41.0, 108.9, 117.6, 120.3, 122.8, 126.3, 126.5, 126.8, 128.3, 135.8, 135.8, 137.0, 139.4, 141.8, 146.9, 148.1, 148.1, 148.4, 154.9, 155.1, 161.7 (Fig. S15). HRMS ( $m/z$ ) calcd. for  $\text{C}_{74}\text{H}_{67}\text{N}_8\text{O}_2$  [ $\text{M}+\text{H}$ ] $^+$ : 1099.5387, found 1099.5393 (Fig. S16).

## 3. Results and discussion

The probe DPPTPy preparation synthetic route is shown below (Scheme 1). Colorimetric and fluorimetric methods were used to confirm the sensing performance of the developed probe. A dual-sensing mechanism established for the metal ion the sensing is via complexation resulting in color change, and for anion (cyanide), it is through addition reaction with a disconnection in intramolecular charge-transfer transition (ICT).

### 3.1. Visual detection

The sensing ability of the DPPTPy probe was studied for naked eye recognition, changes obtained from the probe with various analyte checked visually. In the primary attempt, we tried visible eye detection to discover the sensing ability of DPPTPy ( $2 \times 10^{-5}$  M) towards different cations/anions ( $2 \times 10^{-5}$  M) in a 1:1 DMF:  $\text{H}_2\text{O}$  solution. The chosen analyte (metal ions  $\text{Al}^{3+}$ ,  $\text{Co}^{2+}$ ,  $\text{Cr}^{2+}$ ,  $\text{Cu}^{2+}$ ,  $\text{Sn}^{2+}$ ,  $\text{Hg}^{2+}$ ,  $\text{Fe}^{2+}$ ,  $\text{Fe}^{3+}$ ,  $\text{Mg}^{2+}$ ,  $\text{K}^+$ ,  $\text{Na}^+$ ,  $\text{Ni}^{2+}$ , etc.) and Simple anions like acetate, bromide, chloride, cyanide, fluoride, iodide, nitrate, and phosphate. Selectivity is the essential criterion for sensing. As depicted in Fig. 1, the DPPTPy solution turned to pink for  $\text{Co}^{2+}$ , red for  $\text{Sn}^{2+}$ , and colorless for  $\text{CN}^-$ , from orange color, which denotes high selectivity in the developed probe. Meanwhile, the other cations mentioned above/anions did not yield any substantial color variations. Notably, DPPTPy changed its fluorescence color from bright fluorescence yellowish orange to non-fluorescent for  $\text{Co}^{2+}$ ; non-fluorescent red for  $\text{Sn}^{2+}$ , and in the case of cyanide ion addition, DPPTPy changed its fluorescence color from bright fluorescence yellowish orange to fluorescent blue. Therefore, the developed probe detects multiple ions by producing different colors for each ion ( $\text{Co}^{2+}$ ,  $\text{Sn}^{2+}$ ,  $\text{CN}^-$ ), indicating the probe is selective. In addition, the colorimetric response probes recognition towards anion/cation has been verified and confirmed by a visual detection experiment. The exceptional color change observed for each ion further been confirmed by UV-Visible spectral measurement. The color change of the probe associated with the addition of metal ions due to complexation with pyridine core [42] and for cyanide ion color change occurs due to addition reaction possibility in DPP core, and with the added cyanide ion there exist a disconnection in ICT resulting in colored solution becomes colorless [43].

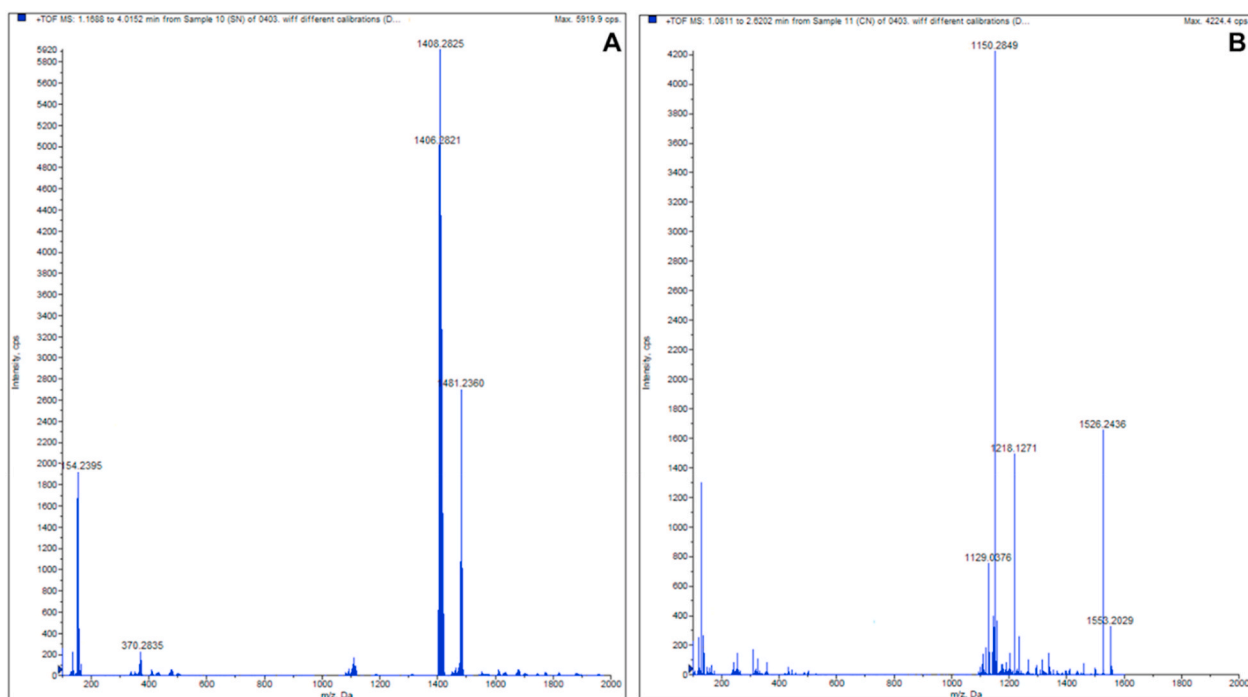
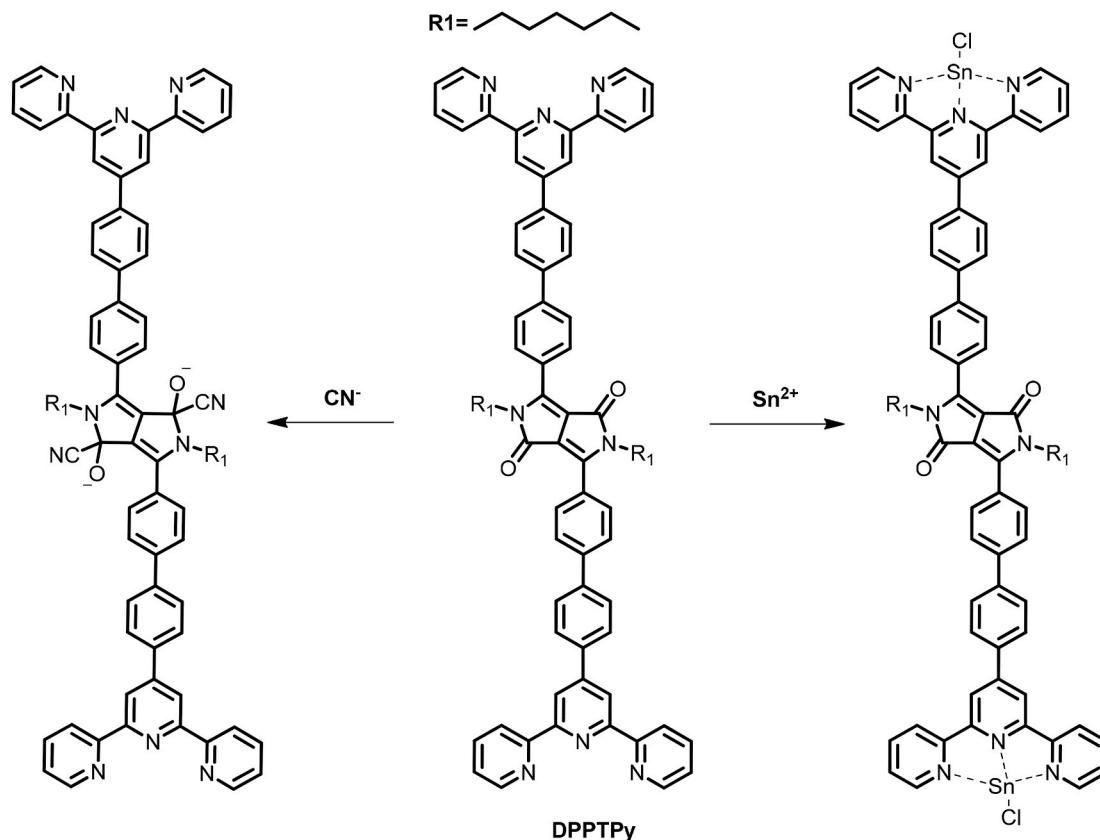


Fig. 6. Binding mass spectra of DPPTPy in the presence of (A)  $\text{Sn}^{2+}$ , and (B)  $\text{CN}^-$ .

### 3.2. UV-visible study

To confirm the changes observed in the visual detection experiment and to agree the sensing ability of probe towards various anion and cation, UV-Visible spectral measurement has been done. As shown in

Fig. 2A, the electronic spectrum of DPPTPy ( $2 \times 10^{-5}$  M) in 1:1 DMF:  $\text{H}_2\text{O}$  solution exhibits an absorbance peak at 283, 322, and broad peak at 491 nm which is because of the  $n-\pi^*$  transition between TPy and DPP core. However, the added  $\text{Co}^{2+}$  ions to a probe solution, the old peaks' intensities enhanced with a shift towards the red region: a broad peak



Scheme 2. Possible binding site of the probe, DPPTPy with  $\text{Sn}^{2+}$  and  $\text{CN}^-$  ion.

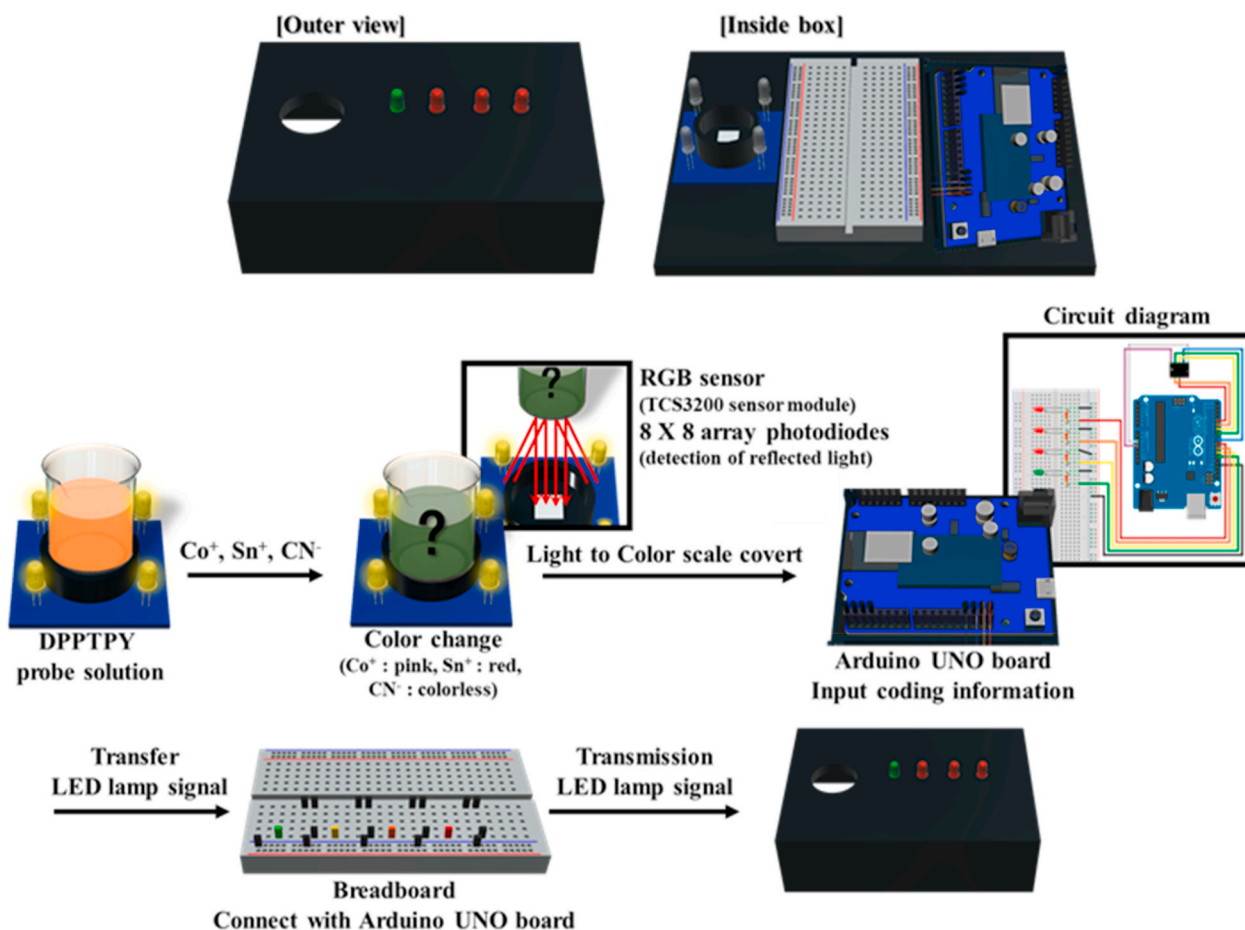


Fig. 7. Graphical illustration of RGB Arduino electronic device, the process takes place in detecting ions.

appeared between 500 and 580 nm. For  $\text{Sn}^{2+}$  ion, the original peak intensities enhanced slightly with a little shift about 8 nm in the absorption spectrum (501 nm) with the color mentioned above change observed in the visual detection experiment. Other cations ( $\text{Al}^{3+}$ ,  $\text{Cr}^{2+}$ ,  $\text{Cu}^{2+}$ ,  $\text{Hg}^{2+}$ ,  $\text{Fe}^{2+}$ ,  $\text{Fe}^{3+}$ ,  $\text{Mg}^{2+}$ ,  $\text{K}^+$ ,  $\text{Na}^+$ ,  $\text{Ni}^{2+}$ , etc.) did not exhibit any substantial absorption and color variations of the probe DPPTPy. Similarly, the anions like acetate, bromide, chloride, fluoride, iodide, nitrate, and phosphate did not yield any substantial absorption variations; only cyanide ion interaction exhibits a disappearance of the original peak at 491 nm (Fig. 2B). The probe's absorption change with added metal ion due to the complexation of the metal ion with pyridine core and cyanide ion, the absorption change due to disconnection in ICT resulting in a colorless solution with no peak at 491 nm.

The binding ability of DPPTPy towards  $\text{Co}^{2+}$ ,  $\text{Sn}^{2+}$ , and  $\text{CN}^-$  was investigated by absorption titration experiment. Upon adding the gradual amount of  $\text{Co}^{2+}$ ,  $\text{Sn}^{2+}$ , and  $\text{CN}^-$  individually to a DPPTPy ( $2 \times 10^{-5}$  M) solution, the ion binding is studied. Three peaks appeared in the probe solution in the 283, 322, and 493 nm regions. While adding  $\text{Sn}^{2+}$  ion ( $0-2 \times 10^{-5}$  M), to the probe solution, peak at 283 nm increased, and a peak appeared in the region of 322 nm disappeared with the formation of a new peak appeared at 349 nm and a shift of original peak at 493–501 nm (Fig. 3A), resulting in a color change of red color from fluorescent orange. With the added cobalt ion ( $0-2 \times 10^{-5}$  M) to DPPTPy solution, the peak at 283 and 322 nm decreased, and peak at 493 nm increased gradually and shifted bathochromic with peak broadening in the range of 520–580 nm (Fig. 3B), and the probe solution changes to pink color. In case of detecting cyanide ion DPPTPy ( $2 \times 10^{-5}$  M) peak appeared at 491 nm intensity reduced gradually with the gradual increase in the cyanide ion ( $0-2 \times 10^{-5}$  M), to the probe resulting a complete disappearance of peak at 491 nm simultaneously peak at 283 and

322 nm decreased and disappeared with formation of a new peak at 297 nm (Fig. 3C). This result demonstrated that the probe DPPTPy effectively detects  $\text{Co}^{2+}$ ,  $\text{Sn}^{2+}$ , and  $\text{CN}^-$  ions.

### 3.3. Fluorescence spectral response

The probe-based on diketopyrrolopyrrole (DPP)-Terpyridine (TPy) derivative individually proved to be a well-known probe as TPy binds effectively with metal ion and cyanide ion easily attacks DPP giving a noticeable color change [42,43]. By combining these two units, the response towards  $\text{Co}^{2+}$ ,  $\text{Sn}^{2+}$ ,  $\text{CN}^-$ , studied by fluorescence technique and other added ion no fluorescence changes were observed (Fig. 4A and B). The development of dual sensing mechanism holding probe is limited, and that too fluorescence quenching effect for metal ions ( $\text{Co}^{2+}$ ,  $\text{Sn}^{2+}$ ) and fluorescence enhancement for anions ( $\text{CN}^-$ ). In the present work, we specially designed the probe DPPTPy for  $\text{Co}^{2+}$ ,  $\text{Sn}^{2+}$ , which has the co-ordination ability with terpyridine (N) as binding sites. With the added metal ion ( $\text{Co}^{2+}$ ,  $\text{Sn}^{2+}$ ) to the DPPTPy ( $2 \times 10^{-5}$  M) solution, fluorescence quenching occurs. To gain better insight into the sensing of DPPTPy for  $\text{Sn}^{2+}$ , a fluorescence titration experiment was employed. DPPTPy reveals substantial peaks at 383 nm & 571 nm when excited at 322 nm (Fig. 5A–C) with stokes shift of 61 nm and 249 nm. With the gradual amounts of  $\text{Sn}^{2+}$  ( $0-2 \times 10^{-5}$  M) addition to DPPTPy, the peak gradually reduced at 383 nm and 571 nm. With the addition of 2 equivalents of  $\text{Sn}^{2+}$  into the DPPTPy solution, peaks seemed at 383 nm, and 571 nm disappeared completely (Fig. 5A). But in the case of  $\text{Co}^{2+}$ , the probes sensing effect via fluorescence technique is spontaneous with even a very low concentration the original peak disappeared with no time (Fig. 5B) such probes are very rare or not reported. In the case of cyanide ion with the gradual amounts of  $\text{CN}^-$  ion ( $0-2 \times 10^{-5}$  M) addition

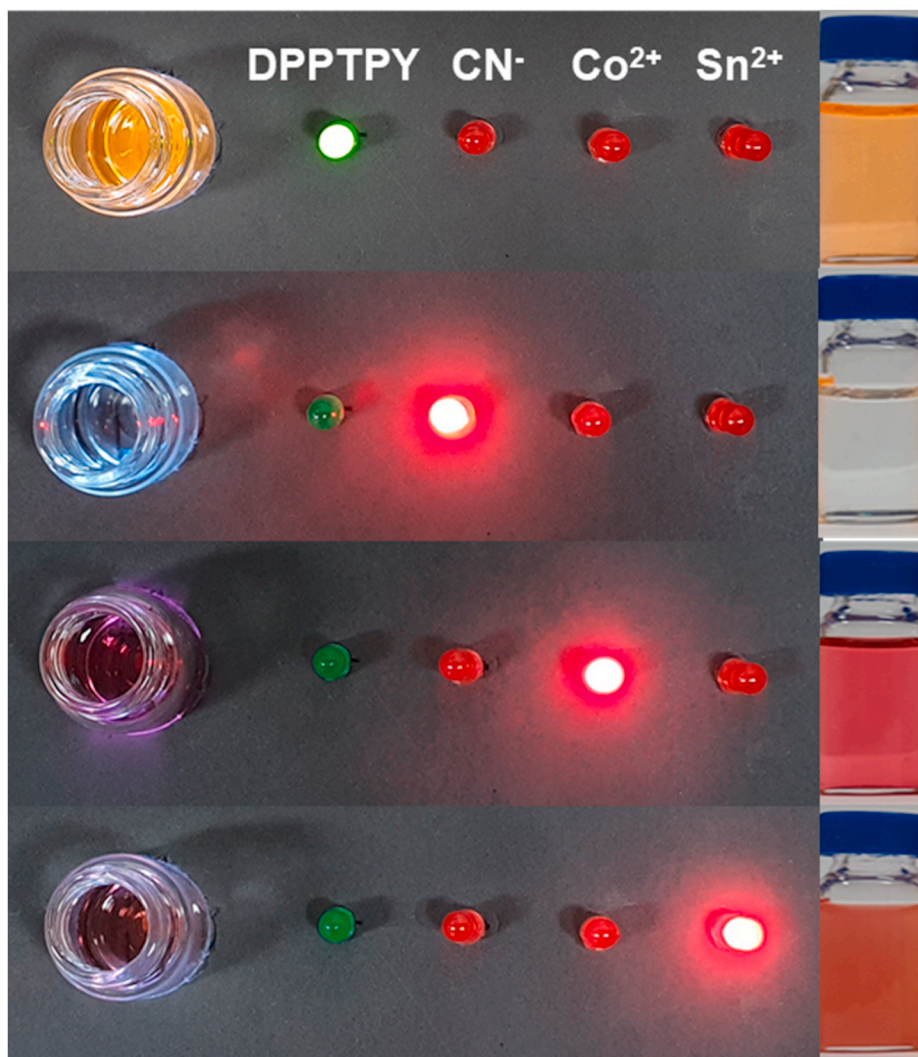


Fig. 8. Response of RGB-Arduino device in detecting  $\text{CN}^-$ ,  $\text{Co}^{2+}$  and  $\text{Sn}^{2+}$  ions.

to DPPTPy, the peak at 383 nm gradually grew, and at the same time, the peak at 571 nm gradually reduced. With the 2 equivalents of  $\text{CN}^-$  into the DPPTPy solution, peak seemed at 571 nm disappeared completely and peak intensity enhanced at 383 nm (Fig. 5C). The data obtained from the fluorescence spectra, the binding constant can be calculated using the equation  $\log [F_0 - F/F] = \log K_A + n \log [\text{Sn}^{2+}]$  (Fig. S17) [44] and found the value as  $4.43 \times 10^8 \text{ M}^{-1}$  for  $\text{Sn}^{2+}$  and for cyanide ion  $(F_\alpha - F_0)/(F_x - F_0) = 1/K[\text{CN}^-]$  it is  $3.08 \times 10^4 \text{ M}^{-1}$  (Fig. S18) [45]. The limit of detection calculated by fluorescence emission spectra and was found to be  $2.21 \times 10^{-9} \text{ M}$  for DPPTPy with  $\text{Sn}^{2+}$  and  $1.44 \times 10^{-8} \text{ M}$  for DPPTPy with  $\text{CN}^-$  by means of  $3\sigma/k$  (Figs. S19 and S20). The quantum yield of the probe DPPTPy before and after adding ions were calculated using the following equation, using quinine sulfate as standard [46]:

$$\Phi_X = \Phi_{\text{ST}} (\text{Grad}_X / \text{Grad}_{\text{ST}}) (\eta_X^2 / \eta_{\text{ST}}^2)$$

Where the subscripts ST and X denote standard and test, respectively,  $\Phi$  is the fluorescence quantum yield, Grad is the gradient from the plot of fluorescence intensity vs absorbance, and  $\eta$  is the refractive index of the solvent. The quantum yield of DPPTPy was found to decrease from 0.49 to 0.09 for  $\text{Sn}^{2+}$  ion and the quantum yield is found to be 0.07 after the addition of cyanide ion. To quantify the stoichiometric ratio between DPPTPy and  $\text{Sn}^{2+}$ , and  $\text{CN}^-$  ion a Job plot measurement was employed (Fig. S21), and the molar fraction of  $[\text{DPPTPy}]/[\text{DPPTPy} + \text{Sn}^{2+}]$  was found to be 0.3, which indicates that the coordination ratio between

DPPTPy and  $\text{Sn}^{2+}$  is approximately 1:2, similarly 1:2 ratio obtained for  $\text{CN}^-$  [39]. Besides, the mass spectral data delivered added proof for the 1:2 compound of DPPTPy- $\text{Sn}^{2+}$ , DPPTPy- $\text{CN}^-$ .

### 3.4. Study of binding mechanism

With the identified stoichiometry from a jobs plot analysis, the binding ability of the probe with the ions ( $\text{Sn}^{2+}$  and  $\text{CN}^-$ ) in the possible binding site was identified further by mass analysis. To know the proper sites of binding of DPPTPy towards  $\text{Sn}^{2+}$  and  $\text{CN}^-$ . A mass spectral analysis experiment done by adding 2 equivalent of the ions mentioned above. The obtained result from the HRMS spectrum of the DPPTPy- $(\text{Sn}^{2+})_2$  (found = 1408.2) complex indicates the expected result (Fig. 6A) and agreed well with the proposed binding site mentioned in Scheme 2. As predicted, the HRMS spectrum of the DPPTPy- $(\text{CN}^-)_2$  (found = 1150.2) complex (Fig. 6B) also agreed well with the proposed binding site. Therefore, from the obtained result, it is confirmed that the DPPTPy dual-sensing mechanism probe for metal ion via complexation and anion (cyanide) is through an addition reaction as illustrated in Scheme 2. Further  $^1\text{H}$  NMR recorded for the probe with cyanide ion and the NMR spectra, which herd the downfield shift of proton peaks corresponding to phenyl near DPP core and the obtained result is shown in (Fig. S22).

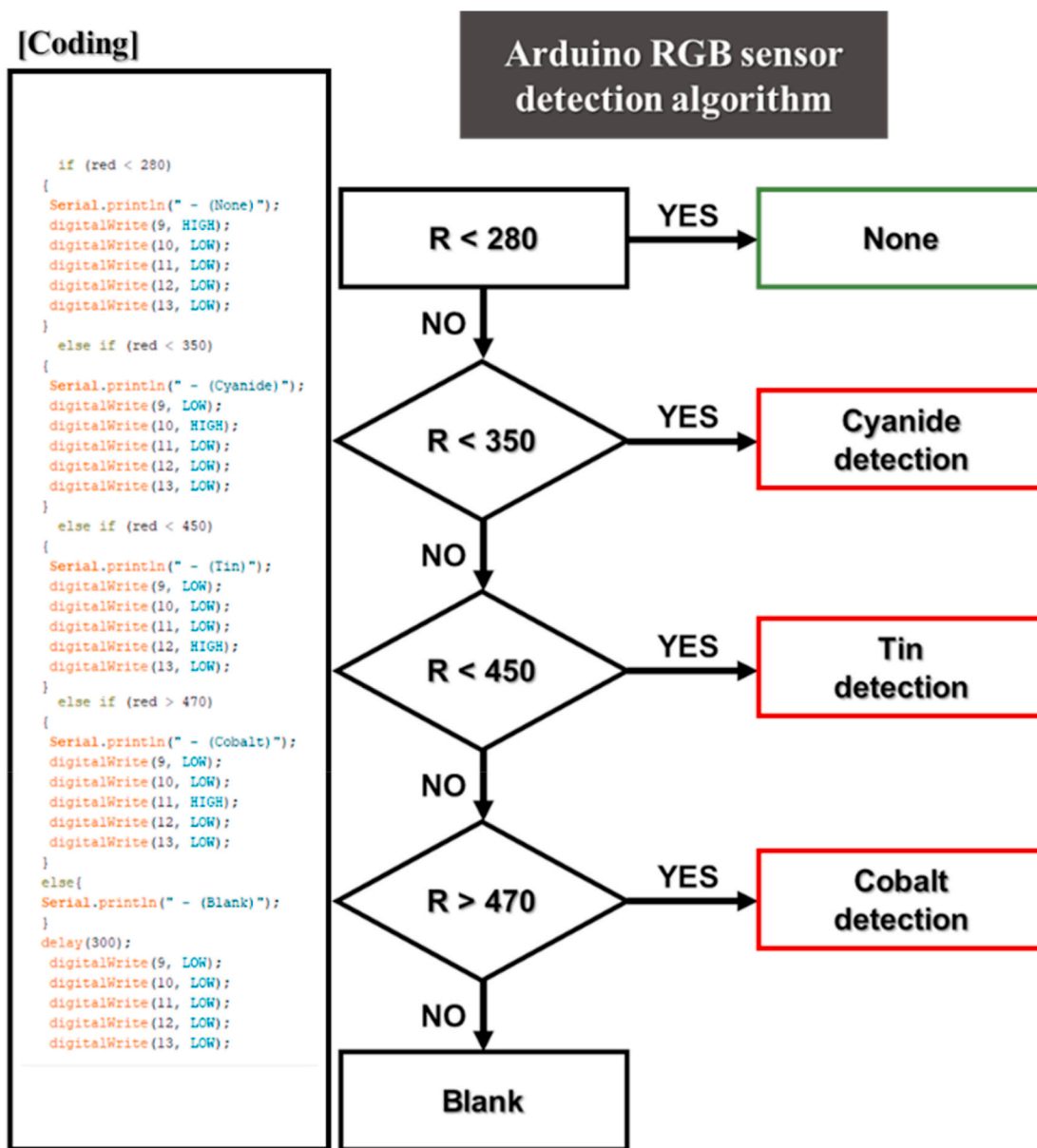


Fig. 9. RGB-Arduino device coding data and algorithm in detecting  $\text{CN}^-$ ,  $\text{Co}^{2+}$  and  $\text{Sn}^{2+}$  ions.

### 3.5. Practical application

#### 3.5.1. An electronic eye (RGB - Arduino device) development and application

RGB sensor kit containing RGB sensor TCS3200 module (Fig. 7): when the metal ion was added to the sample holder vial containing DPPTPY probe illuminates light based on color change and the inner view of the box containing RGB sensor (TCS3200 sensor module, Arduino board, breadboard and LED lamp). The sample (DPPTPY) in the vial is placed in the RGB sensor TCS3200 module. When an ion is added to the DPPTPY probe resulting in a change of color, the module gets different reflection light where light to color scale conversion happens in  $8 \times 8$  array photodiodes. Then, data transfer in USART format will be sent to Arduino board (following coding algorithm) then this information is then passed to the breadboard, and finally the signal is sent to the LED lamp, illuminating light spontaneously. After the successful making of the device, the efficiency of the probe in detection ions was checked.

The probe DPPTPy exhibited diverse colors for the cations ( $\text{Co}^{2+}$ ,

$\text{Sn}^{2+}$ ) and anions ( $\text{CN}^-$ ). Even though the different color obtained for  $\text{Co}^{2+}$  (pink),  $\text{Sn}^{2+}$  (red), but for naked-eye detection, it is hard to distinguish when lower concentration of ion present. To solve this issue an electronic eye developed using RGB Arduino device using TCS3200 sensor module that can easily detect the RGB colors. The device is consisting of an internal photodiode used to read the RGB values. The statistical algorithm created for the developed device also coding data generated for the sensor module. The probe solution ( $2 \times 10^{-5}$  M) was placed in a sample holder; when  $2 \times 10^{-5}$  M solution  $\text{Co}^{2+}$ ,  $\text{Sn}^{2+}$ , or  $\text{CN}^-$  has exposed the probe solution, the color change is determined the RGB Arduino device the obtained result can be monitored and recorded quickly. The obtained result for the ions mentioned above from the device is shown in Fig. 8. The designed algorithm for the RGB - Arduino device and coding data for ion detection given in Fig. 9.

#### 3.5.2. Real sample application

A pre-added selected toxic ions  $\text{Co}^{2+}/\text{Sn}^{2+}$  and  $\text{CN}^-$  100 ppm to the different water samples such as drinking, deionized, tap water (5 mL

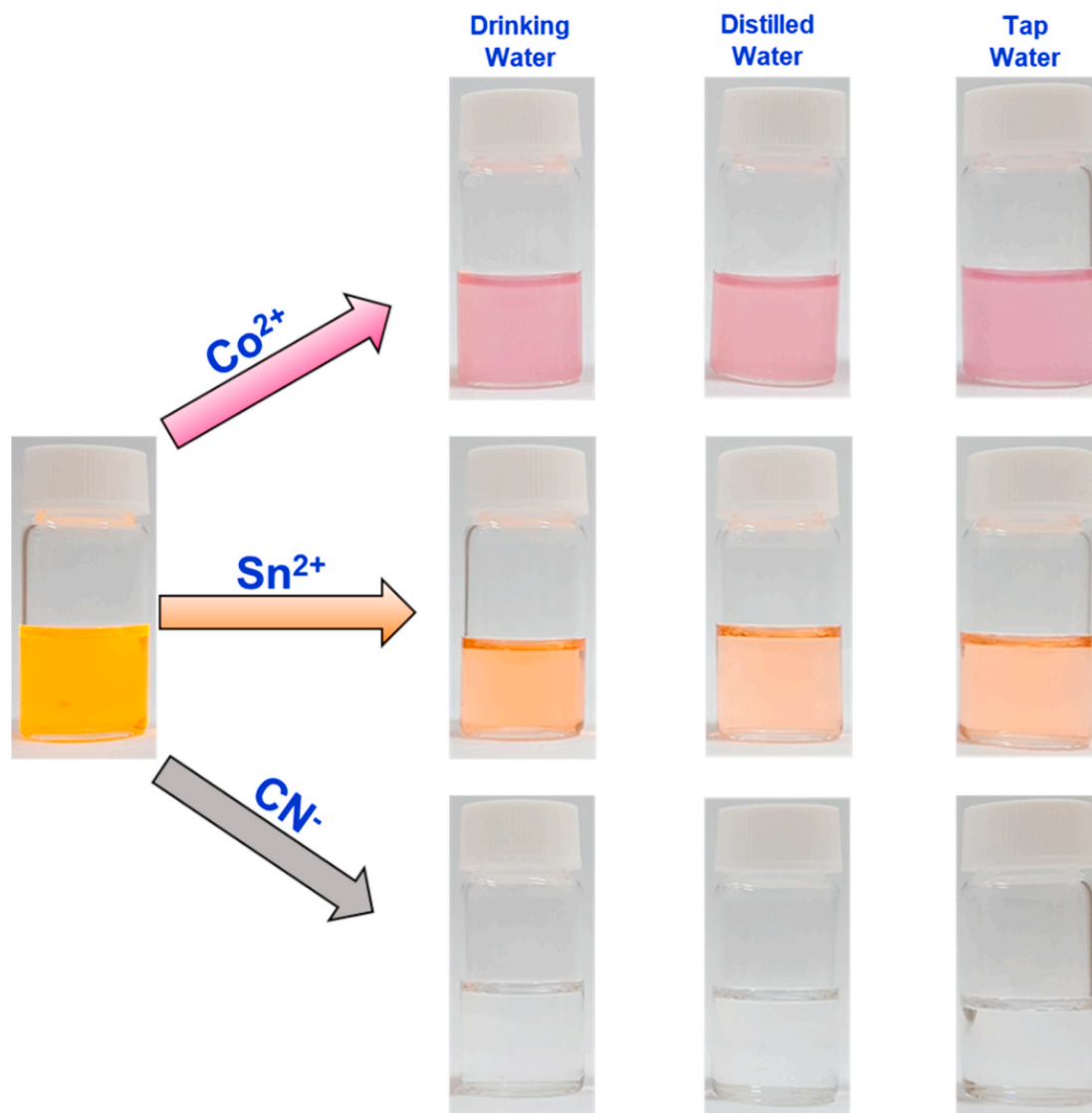


Fig. 10. Visual response of DPPTPY in the presence of  $\text{Sn}^{2+}$ ,  $\text{Co}^{2+}$ , and  $\text{CN}^-$  ion in drinking, distilled and tap water.

approximately), and the ion containing water sample added to the 5 mL of probe solution ( $2 \times 10^{-5}$  M) to each vial. The changes observed in the probe solution are carefully monitored. An immediate color change was observed in each vial indicates the probe DPPTPY effectively detects the aforementioned ions with a different color: pink for  $\text{Co}^{2+}$ , red for  $\text{Sn}^{2+}$  and colorless for  $\text{CN}^-$ , which is originally orange in color. The obtained result is shown in Fig. 10.

#### 4. Conclusion

In summary, a dual sensing mechanism probe for the detection of toxic  $\text{Co}^{2+}/\text{Sn}^{2+}$  and  $\text{CN}^-$  ions in water based on a diketopyrrolopyrrole (DPP) and terpyridine (TPy) fused moiety was designed and well synthesized. Colorimetric response with different color was achieved for  $\text{Co}^{2+}/\text{Sn}^{2+}$  and  $\text{CN}^-$ . A dual-sensing mechanism is confirmed for anion (cyanide), and it is through an addition reaction in the DPP unit with a disconnection in intramolecular charge-transfer transition (ICT). For the metal ion sensing via complexation in TPy unit resulting in color (different) change. A pre-added selected ion to the different water samples effectively detects a different color. In addition, we developed an electronic eye (RGB - Arduino device) for the effective detection of toxic ions.

#### CRediT authorship contribution statement

**Ramalingam Manivannan:** Conceptualization, Methodology, Investigation, Formal analysis, Visualization, Writing – original draft. **Jiwon Ryu:** Investigation, Formal analysis, Investigation, Chromatography experiments, Analyzing data. **Young-A Son:** Conceptualization, Methodology, Supervision, Writing – review & editing.

#### Declaration of competing interest

The authors declare that they have no known competing financial interests or personal relationships that could have appeared to influence the work reported in this paper.

#### Acknowledgements

This research was supported by Chungnam National University (2020-2021).

#### Appendix A. Supplementary data

Supplementary data to this article can be found online at <https://doi.org/10.1016/j.dyepig.2021.109425>.

## References

- [1] Ayangbenro S, Babalola OO. A new strategy for heavy metal polluted environments: a review of microbial biosorbents. *Int J Environ Res Publ Health* 2017;14: 94–09.
- [2] Aron AT, Ramos-Torres KM, Cotruvo Jr JA, Chang CJ. Recognition- and reactivity-based fluorescent probes for studying transition metal signaling in living systems. *Acc Chem Res* 2015;48:2434–42.
- [3] Liu X, Lin Q, Wei TB, Zhang YM. A highly selective colorimetric chemosensor for detection of nickel ions in aqueous solution. *New J Chem* 2014;38:1418–23.
- [4] Cheah PW, Heng MP, Izati A, Ng CH, Tan KW. Rhodamine B conjugate for rapid colorimetric and fluorimetric detection of aluminium and tin ions and its application in aqueous media. *Inorg Chim Acta* 2020;512:119901.
- [5] Vashisht D, Kaur K, Jukaria R, Vashist A, Sharma S, Mehta SK. Colorimetric chemosensor based on coumarin skeleton for selective naked eye detection of cobalt (II) ion in near aqueous medium. *Sens Actuators B Chem* 2019;280:219–26.
- [6] Wang L, Gong X, Bing Q, Wang G. A new oxadiazole-based dual-mode chemosensor: colorimetric detection of  $\text{Co}^{2+}$  and fluorometric detection of  $\text{Cu}^{2+}$  with high selectivity and sensitivity. *Microchem J* 2018;142:279–87.
- [7] Park JH, Manivannan R, Jayasudha P, Son YA. Selective detection of cyanide ion in 100% water by indolium based dual reactive binding site optical sensor. *J Photochem Photobiol Chem* 2020;397:112571.
- [8] Park JH, Manivannan R, Jayasudha P, Son YA. Spontaneous optical response towards cyanide ion in water by a reactive binding site probe. *Spectrochim Acta A* 2020;233:118190.
- [9] Beer P, Gale P. Anion recognition and sensing: the state of the art and future perspectives. *Angew Chem Int Ed* 2001;40:486–516.
- [10] Cheng X, Li H, Zheng F, Lin Q, Zhang Y, Yao H, Wei T. A pillar[5]arene-based cyanide sensor bearing on a novel cyanide-induced self-assemble mechanism. *Dyes Pigments* 2016;127:59–66.
- [11] Ullmann encyclopedia of industrial chemistry. New York: Wiley-VCH; 1999.
- [12] Bhattacharya R, Flora SJS. In: Gupta RC, editor. In handbook of toxicology of chemical warfare agents. Academic Press Boston; 2009.
- [13] Fawell JK. Guidelines for drinking water quality, vol. 1. Geneva: World Health Organization; 1993.
- [14] Liu Z, Jia X, Bian P, Ma Z. A simple and novel system for colorimetric detection of cobalt ions. *Analyst* 2014;139:585–8.
- [15] Maiga A, Diallo D, Bye R, Paulsen BS. Determination of some toxic and essential metal ions in medicinal and edible plants from Mali. *J Agric Food Chem* 2005;53: 2316–21.
- [16] Zhang Z, Zhang J, Lou T, Pan D, Chen L, Qu C, Chen Z. Label-free colorimetric sensing of cobalt(II) based on inducing aggregation of thiosulfate stabilized gold nanoparticles in the presence of ethylenediamine. *Analyst* 2012;137:400–5.
- [17] Battaglia V, Compagnone A, Bandino A, Bragadin M, Rossi CA, Zanetti F, Colombatto S, Grillo MA, Toninello A. Cobalt induces oxidative stress in isolated liver mitochondria responsible for permeability transition and intrinsic apoptosis in hepatocyte primary cultures. *Int J Biochem Cell Biol* 2009;41:586–94.
- [18] Czarnek K, Terpiłowska S, Siwicki AK. Selected aspects of the action of cobalt ions in the human body. *Cent Eur J Immunol* 2015;40:236–42.
- [19] Fawell JK, Ohanian E, Giddings M, Toft P, Magara Y, Jackson P. Inorganic tin in drinking-water. WHO guidelines for drinking-water quality. 2004.
- [20] Wang S, Fei X, Guo J, Yang Q, Li Y, Song Y. A novel reaction-based colorimetric and ratiometric fluorescent sensor for cyanide anion with a large emission shift and high selectivity. *Talanta* 2016;148:229–36.
- [21] Kulig KW. Cyanide toxicity. US Department of Health and Human Services Atlanta GA; 1991.
- [22] Vennesaland B, Comm EE, Knowlens CJ, Westly J, Wissing F. Cyanide in biology. Academic Press London; 1981.
- [23] Hu JW, Lin WC, Hsiao SY, Wu YH, Chen HW, Chen KY. An indanedione-based chemodosimeter for selective naked-eye and fluorogenic detection of cyanide. *Sens Actuators, B* 2016;233:510–9.
- [24] Li J, Qi X, Wei W, Zuo G, Dong W. A red-emitting fluorescent and colorimetric dual-channel sensor for cyanide based on a hybrid naphthopyran-benzothiazol in aqueous solution. *Sens Actuators, B* 2016;232:666–72.
- [25] Wang ST, Sie YW, Wan CF, Wu AT. A reaction-based fluorescent sensor for detection of cyanide in aqueous media. *J Lumin* 2016;173:25–9.
- [26] Sun X, Wang Y, Zhang X, Zhang S, Zhang Z. A new coumarin based chromo-fluorogenic probe for selective recognition of cyanide ions in an aqueous medium. *RSC Adv* 2015;5:96905–10.
- [27] Young C, Tidwell L, Anderson C. Cyanide: social, industrial and economic aspects minerals metals and material society Warrendale. 2001.
- [28] Zhang Q, Zhang J, Zuo H, Wang C, Shen Y. A novel colorimetric and fluorescent sensor for cyanide anions detection based on triphenylamine and benzothiadiazole. *Tetrahedron* 2016;72:1244–8.
- [29] Matsubara K, Akane A, Maseda C, Shiono H. “First pass phenomenon” of inhaled gas in the fire victims. *Forensic Sci Int* 1990;46:203–8.
- [30] Miller GC, Pritsos CA. *Proc Symp Annu Meet TMS* 2001;73.
- [31] Guidelines for drinking-water quality. Geneva Switzerland: World Health Organization; 1996.
- [32] Destanoglu O, Ilmaz GGY, Apak R. Selective determination of free cyanide in environmental water matrices by ion chromatography with suppressed conductivity detection. *J Liq Chromatogr RT* 2015;38:1945–51.
- [33] Minakata K, Nozawa H, Gonmori K, Yamagishi I, Suzuki M, Hasegawa K, Watanabe K, Suzuki O. Determination of cyanide in blood by electrospray ionization tandem mass spectrometry after direct injection of dicyanogold. *Anal Bioanal Chem* 2011;400:1945–51.
- [34] Perring L, Dvorzak MB. Determination of total tin in canned food using inductively coupled plasma atomic emission spectroscopy. *Anal Bioanal Chem* 2002;374: 235–43.
- [35] Shi JX, Lu C, Yan D, Ma L. High selectivity sensing of cobalt in HepG2 cells based on necklace model microenvironment-modulated carbon dot-improved chemiluminescence in Fenton-like system. *Biosens Bioelectron* 2013;45:58–64.
- [36] Tsoutsis D, Guerrini L, Ramon JMH, Giannini V, Marzan LML, Wei A, Puebla RAA. Simultaneous SERS detection of copper and cobalt at ultratrace levels. *Nanoscale* 2013;5:5841–6.
- [37] Khorrami AR, Fakhari AR, Shamsipur M, Naeimi H. Pre-concentration of ultra trace amounts of copper, zinc, cobalt and nickel in environmental water samples using modified C18 extraction disks and determination by inductively coupled plasma-optical emission spectrometry. *Environ Anal Chem* 2009;89: 319–9.
- [38] Kang SM, Jang SC, Kim GY, Lee CS, Huh YS, Roh C. A Rapid in situ colorimetric assay for cobalt detection by the naked eye. *Sensors* 2016;16: 626–6.
- [39] Mahapatra AK, Manna SK, Mandal D, Mukhopadhyay CD. Highly sensitive and selective rhodamine-based “off-on” reversible chemosensor for tin and imaging in living cells. *Inorg Chem* 2013;52:10825–34.
- [40] Dong ZM, Ren H, Wang JN, Chao JB, Wang Y. A new colorimetric and ratiometric fluorescent probe for selective recognition of cyanide in aqueous media. *Spectrochim Acta A* 2019;217:27–34.
- [41] Li J, Chang Z, Pan X, Dong W, Jia AQ. A novel colorimetric and fluorescent probe based on indolium salt for detection of cyanide in 100% aqueous solution. *Dyes Pigments* 2019;168:175–9.
- [42] Lopez MT, Munoz A, Ibeas S, Serna F, Garcia FC, Garcia JM. Colorimetric detection and determination of Fe(III), Co(II), Cu(II) and Sn(II) in aqueous media by acrylic polymers with pendant terpyridine motifs. *Sens Actuators, B* 2016;226:118–26.
- [43] Yang C, Wang X, Xu Z, Wang M. Multi-responsive fluorescence sensing based on a donor-acceptor molecule for highly sensitive detection of water and cyanide. *Sens Actuators, B* 2017;245:845–52.
- [44] Kim IJ, Manivannan R, Son YA. A reaction based colorimetric chemosensor for the detection of cyanide ion in aqueous solution. *Sens Actuators, B* 2017;246:319–26.
- [45] Kim MJ, Manivannan R, Kim IJ, Son YA. A colorimetric and fluorometric chemosensor for the selective detection of cyanide ion in both the aqueous and solid phase. *Sens Actuators, B* 2017;253:942–8.
- [46] Jonathan L, Marco L, Chiara M, Pierpaolo M, Fabio B, Andrea P. N-alkyl diketopyrrolopyrrole-based fluorophores for luminescent solar concentrators: effect of the alkyl chain on dye efficiency”. *Dyes Pigments* 2016;135:154–62.